Journal of the Physical Society of Japan
Vol. 52, No. 8, August, 1983, pp. 2622–2625

Dependence of Loading Resistance and Wave Structures on Plasma Density of ICRF Wave Using Cold Slab Model

Shunjiro SHINOHARA, Masahiro NAITO and Kenro MIYAMOTO

Department of Physics, Faculty of Science, University of Tokyo, Bunkyo-ku, Tokyo 113

(Received May 23, 1983)

Numerical calculation of ICRF wave by cold slab model with a two-ion-species plasma is carried out. This model well explains the dependence of experimental loading resistance on plasma density obtained on TFR, JFT-2, JIPP T-II and TNT-A. The dependence of radial cavity mode on plasma density is also shown.

Heating in ICRF (Ion Cyclotron Range of Frequency)[1] is one of the most promising heating schemes of additional heating. Recently, experimental results have shown high efficiency (3–5 eV/kW/10^{13} cm^{-3}) of ion heating rate with high RF power (<3 MW).[2–5]

It is important to study antenna-plasma coupling and spatial structures from the view point of optimized ICRF heating; antenna configuration and plasma parameters. However, spatial structures of wave field (tunneling, bounded effects and coupling) have not been analyzed until recently, because the analysis is difficult in the case that the wave length of ICRF wave is comparable with the scale length of inhomogeneity of plasma parameters. As ray tracing method[6] fails to describe the wave structures, it is necessary to solve one dimensional stationary wave equation with a boundary condition.[7–9] Although this method with cold plasma assumption cannot treat the mode conversion, and Landau and cyclotron damping, spatial structures of wave field and antenna-plasma coupling can be estimated with good approximation.

Here, we have calculated plasma loading resistance due to antenna-plasma coupling and wave field by the same way as in ref. 7, and compared with the experimental results on TFR,[10] JFT-2,[11] JIPP T-II[12] and TNT-A.*

* S. Shinohara *et al.*: in preparation for publication.

First, we briefly describe the cold slab model. Electromagnetic waves can be excited in the plane wave guide, limited by two walls of infinite conductivity, filled with the plasma. The magnetic field in the z direction varies as $1/(R_0+x)$ in the (x, y, z) co-ordinate system. (R_0: major radius) The parabolic density profile along the x axis is assumed, while the plasma is homogeneous in the y and z direction. Making the Fourier transformation of the antenna current, flows along the y direction on each side of the plasma, in the z direction, differential wave equation for each component with a k_z spectrum can be solved. Then, electromagnetic field distribution for a given current is obtained after making the inverse Fourier transform.

Figure 1 shows the typical example of spatial structure of electric field $|E_y|$ after this calculation at mean plasma density $\bar{n}_e=0.2$ (a) and 1.3×10^{14} cm^{-3} (b) in TFR[10] with the antenna on the high field side. The wave frequency is 70 MHz, toroidal field is 5 T and $n_h/(n_h+n_d)=0.06$. (n_h and n_d are hydrogen and deuterium density, respectively.) In TFR the loop antennae are used and the main fraction of the power couples to the plasma is launched from the high field side. As is well known, two-ion cutoff and two-ion hybrid resonance layer ($x\sim0.05$ m) act as a reflector from the wave coming from the low field side, and as a absorbant from the high field side. Therefore, the eigen mode structure appears between the outer side of the wall and

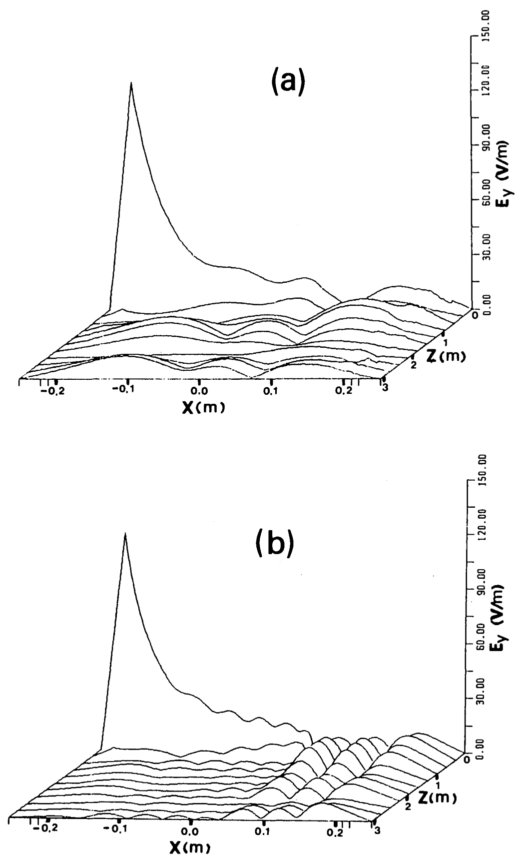

Fig. 1. Spatial structure of electric field $|E_y|$ at mean plasma density $\bar{n}_e=0.2$ (a) and $1.3\times10^{14}\,\mathrm{cm}^{-3}$ (b) in TFR with the antenna current 1 A. (major radius $R_0=98$ cm, minor radius $a_p=21$ cm, antenna radius $a_a=22$ cm, wall radius $a_w=25$ cm, antenna width $w=6$ cm)

two-ion cutoff layer.

Hereafter, we define (m, n) as follows; m is the number of the peak of $|E_y|$ between inner side of the wall and two-ion hybrid resonance layer/two-ion cutoff layer, and n is between outer side of the wall and this layer.

Figure 2 shows the dependence of loading resistance R on mean plasma density $\bar{n}_e$ in TFR with same parameters in Fig. 1. Loading resistance is defined as radiated power of the antenna divided by the square of the current. With the increase in $\bar{n}_e$, R increases with some sharp peaks. The appearance of such peaks is considered to be due to toroidal eigen mode (in z direction). Slow change of loading resistance with plasma density (undulation) is due to radial eigen mode (in x direction);

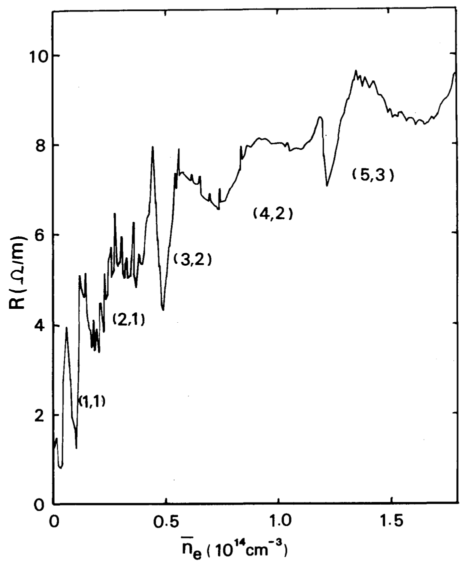

Fig. 2. Dependence of loading resistance R on mean plasma density $\bar{n}_e$ in TFR with same parameters in Fig. 1. Here, (m, n) shown in this figure means that m is the number of peaks of $|E_y|$ between the inner side of the wall and two-ion hybrid resonance layer/two-ion cutoff layer, and n is between the outer side of the wall and this layer.

different (m, n) mode appears when plasma density region is different and mode number increases with plasma density, as shown in Fig. 2. Above $\bar{n}_e\sim7\times10^{13}\,\mathrm{cm}^{-3}$, the effect of toroidal eigen mode structure becomes weak. These phenomena by this calculation explain the experimental results.[10)]

With the increase in plasma density, the maximum k_z value, at which the antenna couples with the plasma, increases; *e.g.*, at $\bar{n}_e=$ 0.3, 0.7, 1.0 and $1.5\times10^{14}\,\mathrm{cm}^{-3}$, the value of the maximum k_z are ~18, 25, 30 and $32\,\mathrm{m}^{-1}$, respectively. It is concluded that high density operation is favourable because loading resistance is higher, toroidal eigen mode structure is weaker (mode tracking is not necessary) and k_z spectrum of antenna-plasma coupling becomes wider.

In Fig. 3, the dependence of loading resistance in JFT-2[11)] with the antenna on the high field side as a function of mean plasma density is shown. Here, R_p means the experimental resistance of antenna-plasma coupling (Vacuum loading resistance is subtracted.) and the wave frequency is 18 MHz. Loading resistance increases slowly with plasma density

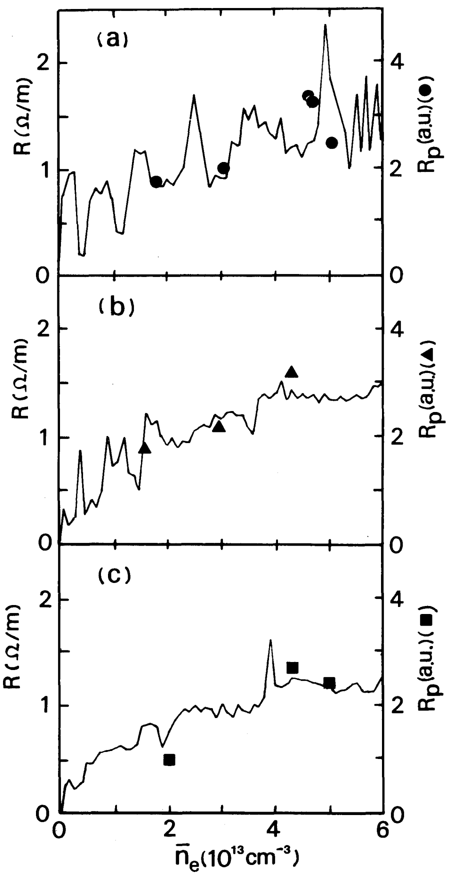

Fig. 3. Dependence of loading resistance R on mean plasma density $\bar{n}_e$ in JFT-2 with $B_t=1.2$ T, $n_h/n_d=4\%$ (a), $B_t=1.25$ T, $n_h/n_d=10\%$ (b) and $B_t=1.5$ T, $n_h/n_d=30\%$ (c). Here, R_p is experimental loading resistance of antenna-plasma coupling. (Vacuum loading resistance is subtracted.) ($R_0=90$ cm, $a_p=25.5$ cm, $a_a=27$ cm, $a_w=30$ cm, $w=4.8$ cm)

and similar results are obtained between experiments and calculation. With the increase in toroidal field and ratio of minority hydrogen to majority deuterium density (from (a) to (c) in Fig. 3), calculation curve becomes smooth.

The distance between plasma and antenna surface becomes far, loading resistance decreases, which agrees well with the experimental results.[11]

Figure 4 shows the relation between loading resistance and mean plasma density for various values of toroidal field in JIPP T-II.[12] Experimental conditions are that wave frequency is 40 MHz and the antenna consists of two half turn coils to which 180 degrees out of phase RF voltages are supplied. Therefore, calculation is done in the case that the current of the antenna, located on the high and low field side, flows opposite direction each other ($m=0$ mode excitation). As shown in Fig. 4, loading resistance depends on plasma density and toroidal field. Increasing toroidal field from 2.52 to 2.71 T, plasma density, at which the value of loading resistance becomes maximum, shifts to higher plasma density. Experimental results are explained by this model and these features indicate the presence of local cavity mode. The ratio of coupling power from high field side to that from low field side are considered. This ratio increases with plasma density, but abrupt decrease is observed near the peak of loading resistance. When plasma density region is far from this peak, this ratio becomes large again.

Absolute value of loading resistance from calculation is larger than that from experiments, and we have not calculated loading resistance in the case of $B_t=2.52$ T because two-ion hybrid resonance layer is absent in the plasma. The value of the maximum k_z to couple with the plasma increases from ~ 10 to $\sim 20\ m^{-1}$ when $\bar{n}_e$ is changed from 1 to 4×10^3 cm^{-3}.

The calculation is also applied to TNT-A[13,14] in the case of low field side excitation using this cold slab model. ($R_0=39.5$ cm, $a_p=7.5$ cm, $a_a=8.0$ cm, $a_w=12$ cm, $w=1.2$ cm) As mean plasma density and toroidal field are relatively low ($\bar{n}_e\sim 10^{13}\ cm^{-3}$ and $B_t\sim 0.4$ T) in this device, the standing wave with half wavelength between the inner and outer side of the wall is observed by this model. The increase in loading resistance with plasma density and effect of the distance between the antenna and plasma surface on loading resistance are calculated and have fairly good agreement with experimental results.

In conclusion, the relation between loading resistance and plasma density is investigated by cold slab model and we have good agreement with the experimental results on TFR, JFT-2, JIPP T-II and TNT-A. The structure of cavity mode is also elucidated. These results are useful for understanding the wave excitation, propagation and damping, and give in-

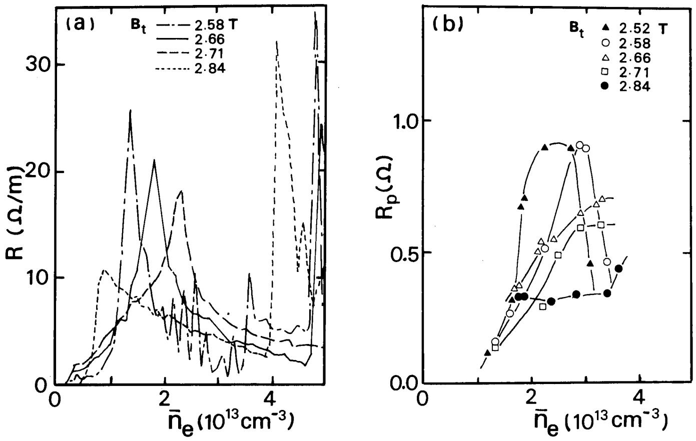

Fig. 4. Relation between loading resistance (R is derived from calculation and R_p is from experiments) and mean plasma density $\bar{n}_e$ for various values of toroidal field in JIPP T-II. (R_0=91 cm, a_p=15 cm, a_a= 16.5 cm, a_w=20 cm, w=7.4 cm)

formation in the case of designing the optimized antenna to couple with the plasma strongly. For precise value of loading resistance and wave structure, we need the two dimensional model with kinetic effects including the collision.

References

1) T. H. Stix: Nucl. Fusion **15** (1975) 737.
2) D. Hwang *et al.*: in *Plasma Physics and Controlled Nuclear Fusion Research* (Proc. 9th Int. Conf., Baltimore, 1982) IAEA-CN41/I-1.
3) TFR Group, A. Trunc, D. Gresillon: *ibid.* IAEA-CN-41/I-2.
4) H. Kimura *et al.*: *ibid.* IAEA-CN-41/J-3.
5) T. Amano *et al.*: *ibid.* IAEA-CN-41/C-3.
6) B. D. McVey: Nucl. Fusion **19** (1979) 461.
7) Y. Lapierre: CEA-Euratom Report, EUR-CEA-FC-1043 (1980).
8) V. P. Bhatnager *et al.*: in *Plasma Physics and Controlled Nuclear Fusion Research* (Proc. 9th Int. Conf., Baltimore, 1982) IAEA-CN-41/J-2.
9) A. Fukuyama, S. Nishiyama, K. Itoh and S. I. Itoh: Research Report HIFT-68 (Institute for Fusion Theory, Hiroshima University) (1982).
10) Equipe TFR: CEA-Euratom Report, EUR-CEA-FC-1115 (1981).
11) H. Kimura *et al.*: JAERI-M 82–046 (1982).
12) M. Ichimura *et al.*: Proc. Int. Conf. on Plasma Phys. **1** (1982) 125.
13) S. Shinohara, K. Sakuma, Y. Nagayama, H. Toyama: J. Phys. Soc. Jpn. **52** (1983) 94.
14) S. Shinohara, I. Ochiai, S. Tsuji, H. Toyama, K. Miyamoto: J. Phys. Soc. Jpn. **52** (1983) 364.